

引用格式: LI Jianhui, YANG Chunmei, ZHANG Caifeng, et al. Preparation of ZnO/BiOBr Composites and Photocatalytic Degradation of RhB under Visible Light[J]. Acta Photonica Sinica, 2022, 51(2):0216001

李建会, 杨春梅, 张彩凤, 等. ZnO/BiOBr 复合材料制备及可见光催化降解 RhB 性能研究[J]. 光子学报, 2022, 51(2):0216001

ZnO/BiOBr 复合材料制备及可见光催化降解 RhB 性能研究

李建会¹, 杨春梅¹, 张彩凤^{1,2}, 张申¹, 马小红¹, 吴晓婧¹, 王田业¹,
岳秀丽¹, 常敏冉¹

(1 太原师范学院 化学系, 山西 晋中 030619)

(2 山西省有机旱作农业肥料工程研究中心, 山西 晋中 030619)

摘 要:通过溶剂热法制备不同 ZnO 和 BiOBr 摩尔配比的 ZnO/BiOBr 复合光催化剂。ZnO 与 BiOBr 摩尔比为 1:2 时, ZnO/BiOBr 复合材料光催化降解罗丹明 B 的性能最好, 可见光照 120 min, 罗丹明 B (20 mg/L) 去除率达 98.89%, 降解速率常数为 $0.040\ 50\ \text{min}^{-1}$, 是纯 BiOBr 的 4 倍。紫外-可见漫反射和荧光光谱分析显示较纯 ZnO, ZnO/BiOBr(1:2) 吸收带红移, 光子利用率提高, 且光生电子-空穴复合机率降低。通过电子顺磁共振波谱仪和半导体能带理论对降解机理进行分析, 结果显示降解过程主要通过 $\cdot\text{O}_2^-$ 、 $\cdot\text{OH}$ 自由基的氧化作用, ZnO 与 BiOBr 之间形成界面电场, 降低了电子-空穴的复合机会。

关键词:光催化; 光子; 降解; ZnO/BiOBr; 罗丹明 B

中图分类号: O643

文献标识码: A

doi: 10.3788/gzxb20225102.0216001

0 引言

纺织、印染、涂层、医药等工业生产活动过程中, 约有 10%~15% 的有机污染物会伴随着工业废水被排放进入周围的水体、土壤和大气中^[1-3], 增加了有机染料治理的难度。较为成熟的传统工业废水治理方法有物理方法(主要包括吸附、膜过滤等)、化学方法(电化学氧化法等)以及生物化学法等。1972 年, FUJISHIMA A 等首次发现采用 TiO₂ 铂电极构成的光电化学体系在紫外光照的激发下, 水会分解生成氢气^[4]。基于这一反应原理, 光催化技术开始被用来降解有机污染物, 也逐渐被人们认为是解决未来能源短缺和环境污染问题最有发展前景的技术之一。

然而, 光催化剂的应用仍然存在许多问题, 如光子效率低、光诱导电子-空穴对复合率高或稳定性差等^[5]。为了扩大光催化技术的工业应用, 对光催化剂改性是提高太阳能利用率的重要方向。ZnO 具有光敏性好、无毒性、电子迁移率高、成本低等优点^[6], 但其属于宽带隙半导体, 只对紫外光响应^[7], 光子利用率低。

氧化卤化铋 BiOX(X=Cl, Br, I) 因其特殊的结构和优良的光催化性能, 受到广泛关注。其中, BiOBr 作为一种典型的卤氧化铋光催化剂, 具有合适的带隙(2.61 eV), 使得它在可见光的照射下具有活性好、光催化性能稳定的特点, 所以它在光催化降解水污染的领域里成为不可忽视的材料之一^[8]。但是纯 BiOBr 的光催化效果较差, 采取 BiOBr 与 ZnO 复合的方式, 形成 BiOBr/ZnO 异质结, 可提高单组份半导体光催化材料的光催化剂活性, 拓宽 ZnO 和 BiOBr 的使用范围^[9]。

以往研究采用水热法合成二元复合材料 ZnO/BiOBr, 进行染料的降解实验探究, 提高了单组份的光催化降解活性。SHASHA Y 等^[10]采用两步水热法制备了 ZnO/BiOBr 复合物, 对甲基橙(MO)光降解表现出

基金项目: 太原师范学院 2021 年大学生创新创业训练项目(No. CXCY2138), 山西省“1331 工程”协同创新中心建设计划(No. 11703200)

第一作者: 李建会(1988—), 女, 讲师, 博士, 主要研究方向为水污染控制及资源化利用。Email: lijianhui1699@163.com

收稿日期: 2021-08-10; 录用日期: 2021-10-14

<http://www.photon.ac.cn>

优异的催化活性。GENG Y G等^[11]采用水剂热法合成类花球状ZnO/BiOBr,对甲基蓝(MB)呈现良好的光催化降解能力。MENG X C等^[12]采用水热法合成二元异质结ZnO/BiOBr,对罗丹明B(Rhodamine B, RhB)的光降解能力明显优于单组份。

本课题采用添加部分乙二醇溶剂的方式,一步溶剂热法合成与以往不同形貌的ZnO/BiOBr,虽然因反应条件和降解底物不同,无法对比光催化活性,但筛选出高催化降解活性的ZnO/BiOBr(1:2)。并使用电子顺磁共振波谱仪(Electron Spin Resonance, ESR)和半导体能带理论对降解机理进行系统分析,确定无选择性 $\cdot\text{O}_2^-$ 、 $\cdot\text{OH}$ 自由基的产生和ZnO/BiOBr(1:2)光催化降解机理。

1 实验部分

1.1 光催化剂ZnO/BiOBr的制备

实验所用药品均为分析纯,采用溶剂热法合成ZnO/BiOBr,首先将KOH和 $\text{Zn}(\text{NO}_3)_2 \cdot 6\text{H}_2\text{O}$ (两者摩尔比为2)溶于30 mL去离子水中,形成 $\text{Zn}(\text{OH})_2$ 的悬浮液,然后边搅拌边向悬浮液中加入一定量的KBr,得到混合液A;再将8 mmol $\text{Bi}(\text{NO}_3)_3 \cdot 5\text{H}_2\text{O}$ 溶于30 mL的乙二醇,得到B溶液,随后将B溶液缓慢加入混合液A中,最后将混合液转移至含有聚四氟乙烯内衬的高压反应釜中,于120 °C下反应12 h,冷却至室温后分别用乙醇、去离子水洗涤三次,所得ZnO/BiOBr(两者的摩尔比分别为1:1、1:2、1:3、2:1、2:3、3:1、3:2)产物在70 °C的鼓风干燥箱中干燥12 h。制备过程中ZnO与BiOBr的摩尔比通过 $\text{Zn}(\text{NO}_3)_2 \cdot 6\text{H}_2\text{O}$ 和 $\text{Bi}(\text{NO}_3)_3 \cdot 5\text{H}_2\text{O}$ 摩尔量进行调控。

1.2 光催化性能的测试

取100 mL 20 mg/L的罗丹明B溶液,向其中加入0.030 g催化剂样品,在避光状态下均速磁力搅拌混合溶液1 h,使得催化剂与罗丹明B之间基本建立吸附-脱附平衡后,进行光催化降解实验。光源由中教金源500 W的氙气灯提供,光源与降解液液面距离为15 cm,光照一定时间后取降解液于紫外-可见分光光度计554 nm处进行吸光度测试,通过标准曲线计算对应的浓度,计算出不同光照时间下RhB的降解程度,即

$$y = \frac{C_t}{C_0} \times 100\% \quad (1)$$

式中, C_0 表示初始浓度, C_t 为光照时间 t 时RhB溶液的浓度。

1.3 样品表征

采用日本理学MiniFlex600进行X射线衍射(X-Ray Diffraction, XRD)分析,扫面范围为 $10^\circ \sim 80^\circ$;用日本日立公司扫描电子显微镜(Scanning Electron Microscopy, SEM, 仪器型号JSM-IT200)和透射电镜(Transmission Electron Microscopy, TEM, 仪器型号FEI Tecnai F30)观察样品的形貌和组成;用紫外-可见漫反射光谱(UV-vis Diffuse Reflection Spectroscopy, UV-Vis DRS, Lambda1050)分析样品的吸收光边带和禁带宽度,扫面范围为200~800 nm;采用爱丁堡仪器F7100采集样品的荧光光谱,激发波长为325 nm,扫描范围为360~800 nm;采用日本电子株式会社的电子顺磁共振波谱仪分析(ESR, JES-FA200)分析光催化降解过程中自由基 $\cdot\text{O}_2^-$ 和 $\cdot\text{OH}$ 的产生情况,使用5,5-二甲基-1,1-吡咯啉-N-氧化物(DMPO)进行自由基的捕获,分别于水体和甲醇体系中检测。

2 结果与讨论

2.1 催化剂的分析表征

2.1.1 XRD

图1显示了ZnO、BiOBr和ZnO/BiOBr的XRD谱图,三种样品XRD的衍射峰窄而尖锐,说明三种样品均具有良好的结晶度。从图中可清楚地看到ZnO样品符合六方纤锌矿结构(JCPD NO. 36-1451),纯BiOBr样品与BiOBr四方晶体结构(JCPDS 78-0348)一致^[11]。ZnO和BiOBr以1:2摩尔比合成二元材料ZnO/BiOBr(1:2),ZnO/BiOBr(1:2)的XRD衍射峰表现出六方纤锌矿ZnO和四方BiOBr晶体相共存,说明两者成功复合。

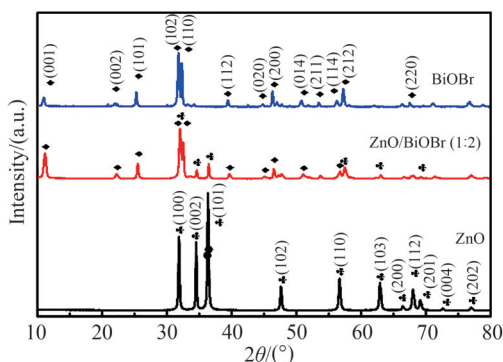


图1 ZnO、BiOBr和 ZnO/BiOBr的 XRD 谱

Fig.1 XRD spectrogram of ZnO, BiOBr and ZnO/BiOBr (1:2)

2.1.2 扫描电镜分析

扫描电镜图清楚地显示了不同 ZnO/BiOBr 配比样品的形貌。图 2(a)和(b)显示了纯 ZnO 和 BiOBr 分别为颗粒状和薄片状结构。ZnO 与 BiOBr 配比为 3:1, 2:1 和 3:2 时,如图 2(c)~(e),二元复合材料 ZnO/BiOBr 结构的表面可以明显看到 ZnO 颗粒附着在片状结构的表面,随着 ZnO 摩尔配比减少,二元复合材料 ZnO/BiOBr 呈现不同尺寸的片状结构,且片状结构的表面看不到颗粒状 ZnO 的存在,其中 ZnO/BiOBr (1:2)(图 2(h))样品的片状结构尺寸最大。

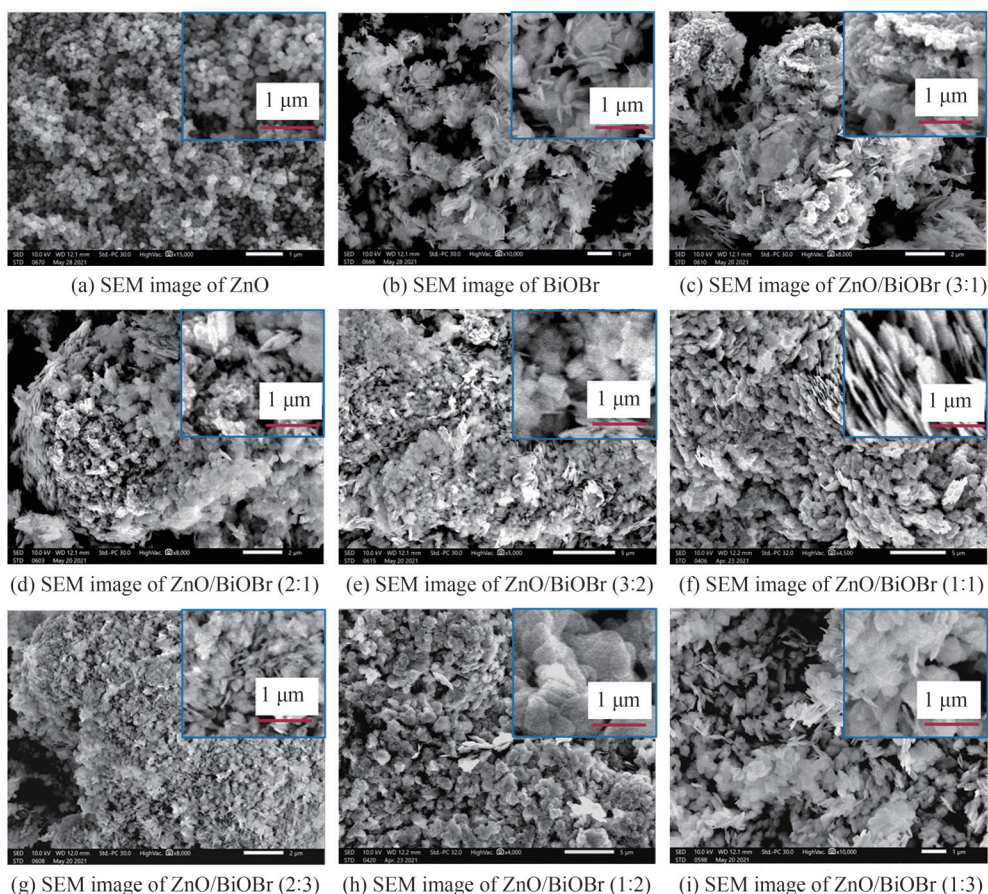


图2 样品的扫描电镜图

Fig.2 The SEM images of samples

2.1.3 透射电镜分析

TEM分析中,图 3能清楚显示 ZnO/BiOBr (1:2)的片状结构,尺寸大小不一,但这种薄片结构包含大量的间隙,利于光射到催化剂的内部以及光生载流子的传递。HR-TEM(图 3(b))显示样品清晰的晶格条纹,

黄线圈内区域晶格条纹的晶格间距为0.285 nm,与BiOBr(102)面相吻合,红线圈内区域晶格条纹的间距为0.264 nm,与ZnO(002)面相匹配,证明ZnO和BiOBr成功形成异质结。

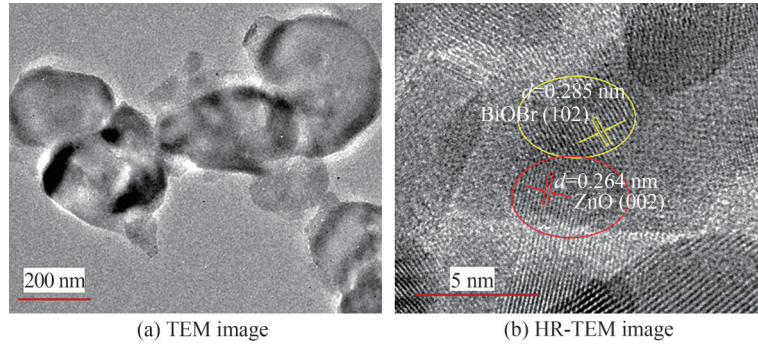


图3 ZnO/BiOBr (1:2)样品的TEM图
Fig.3 The TEM images of ZnO/BiOBr (1:2) sample

2.1.4 UV-Vis DRS 分析

通过紫外-可见漫反射和荧光光谱分析ZnO、ZnO/BiOBr (1:2)和BiOBr样品的光学性能。从图4(a)中可以看到纯ZnO的吸收光边缘位于400 nm以内(约395 nm),间接说明ZnO对可见光无响应,这与文献报道^[10-12]一致。纯BiOBr的吸收光边缘位于约454 nm处,ZnO和BiOBr复合形成二元材料ZnO/BiOBr (1:2),其吸收光边缘位于约445 nm处,说明ZnO/BiOBr (1:2)具有可见光响应,ZnO和BiOBr复合后较纯ZnO,复合材料的吸收光边缘向低能区移动(红移),更利于光子激发,对光的吸收能力增强,可提高太阳光利用率^[13-14]。

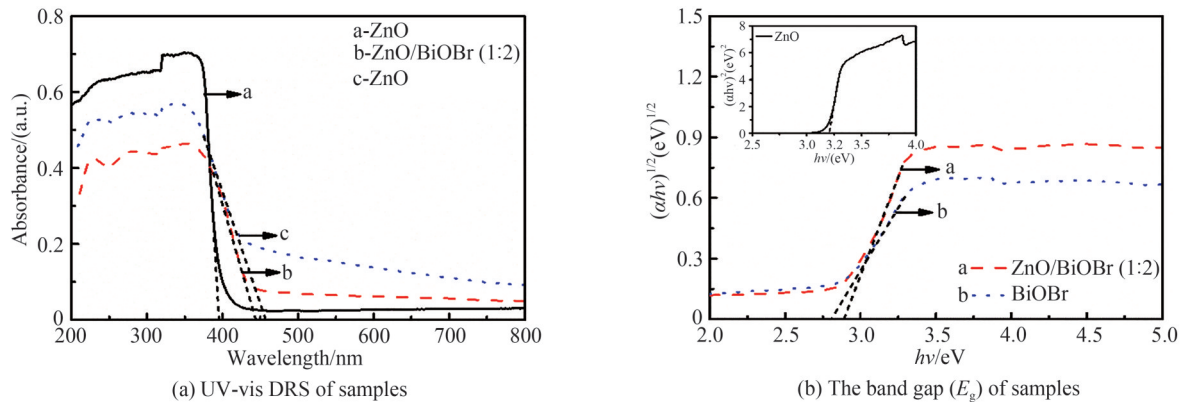


图4 ZnO、ZnO/BiOBr (1:2)和BiOBr的UV-vis DRS分析
Fig.4 UV-vis DRS of ZnO, ZnO/BiOBr (1:2) and BiOBr

根据样品的紫外-可见漫反射谱图,禁带宽度 E_g 计算公式为^[15]

$$ah\nu = A(h\nu - E_g)^{1/2} \quad (2)$$

式中, α 、 h 、 ν 、 E_g 和 A 分别是光学吸收系数、普朗克常数、光频率、带隙能量和比例常数。BiOBr为间接带隙半导体, n 值为4,ZnO是直接带隙半导体, n 值为1。

通过作图(图4(b))分析ZnO、ZnO/BiOBr (1:2)和BiOBr的禁带宽度分别为3.21、2.90和2.80 eV,虽然二元复合材料ZnO/BiOBr (1:2)禁带宽度稍大于纯BiOBr,但较纯ZnO,BiOBr与ZnO复合后,禁带宽度明显减小,说明对光谱的利用范围提升,这对光催化性能的提升有利。

2.1.5 荧光光谱分析

荧光光谱分析用于说明光生电子-空穴的去向,判断光生电子-空穴复合机率的大小,荧光光谱峰越强,电子-空穴的复合率越大,与之对应的光生电子-空穴的利用率就越低,越不利于光催化效率的提高^[16]。ZnO属于缺陷发光,BiOBr属于带隙发光。图5结果显示纯ZnO的光谱峰强最强,说明ZnO光生电子-空穴

的复合机率最大,即光生电子-空穴的利用率最低;纯BiOBr的峰强最弱,说明BiOBr光生电子-空穴的复合几率最小;二元复合材料ZnO/BiOBr(1:2)峰强介于纯ZnO和BiOBr之间,说明BiOBr的加入提高了纯ZnO的光生电子-空穴的利用率。

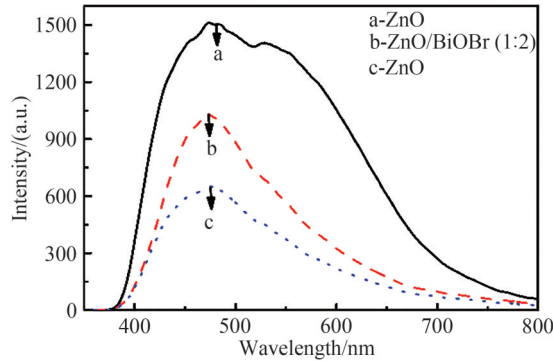
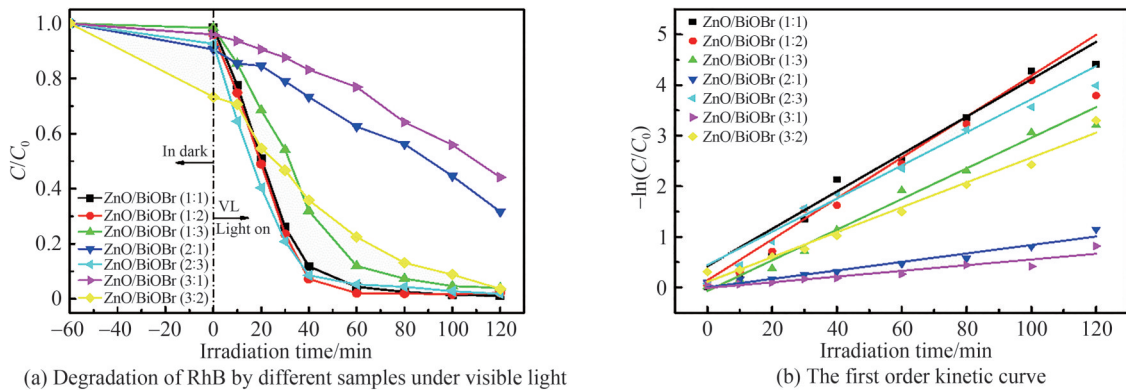


图5 ZnO、ZnO/BiOBr(1:2)和BiOBr的荧光光谱
Fig.5 Fluorescence spectra of ZnO, ZnO/BiOBr(1:2)和BiOBr

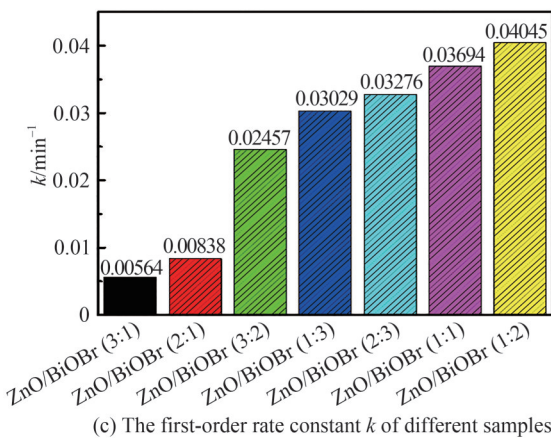
2.2 光催化活性评价

图6(a)为ZnO/BiOBr复合光催化剂在可见光的照射下对罗丹明B的降解曲线,单组分ZnO对可见光无响应,因此在可见光照射下,罗丹明B不降解,实验也验证了这个结果。在前期工作中,已经对单组分BiOBr的降解活性进行了研究^[16],光照120 min,罗丹明B降解74.71%,一级动力学常数为0.01 min⁻¹。由图6(a)可看到在相同条件下,不同配比的ZnO/BiOBr复合材料对罗丹明B的降解效果是不一样的,光照120 min,ZnO/BiOBr(1:1)、ZnO/BiOBr(1:2)、ZnO/BiOBr(1:3)、ZnO/BiOBr(2:3)、ZnO/BiOBr(3:2)、

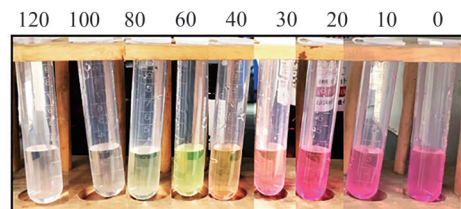


(a) Degradation of RhB by different samples under visible light

(b) The first order kinetic curve



(c) The first-order rate constant k of different samples



(d) Change of RhB solution color with time under ZnO/BiOBr(1:2)

图6 光催化降解实验

Fig.6 Photocatalytic degradation experiment

ZnO/BiOBr (2:1)、ZnO/BiOBr (1:3)对罗丹明B的降解率分别为98.8%、97.8%、96.0%、98.2%、96.3%、68.3%和55.8%,从结果看到,适当的ZnO和BiOBr摩尔比可以合成高活性二元复合材料,ZnO占比过多对二元复合材料ZnO/BiOBr光催化性能的提升不利。ZnO/BiOBr (1:2)对罗丹明B的降解率是纯BiOBr的1.31倍。

为了进一步分析不同配比复合光催化剂ZnO/BiOBr对罗丹明B的降解能力,对光催化过程拟合动力学曲线,从分析结果显示,此降解基本符合一级动力学曲线,即

$$-\ln(C_0/C_t)=kt \quad (3)$$

式中, k 为降解速率常数(min^{-1}), C_0 为降解液的初始浓度(mol/L), C_t 为经过光照时间 t 的降解液浓度(mol/L)。

以 $-\ln(C_0/C_t)$ 为纵坐标,光照时间 t 为横坐标进行线性拟合,可以得到各催化剂的降解速率常数 k (图6(b))。将不同样品的 k 值汇总于图6(c)中,不同样品的反应速率常数 k 值大小依次为ZnO/BiOBr (1:2) > ZnO/BiOBr (1:1) > ZnO/BiOBr (2:3) > ZnO/BiOBr (1:3) > ZnO/BiOBr (3:2) > ZnO/BiOBr (2:1) > ZnO/BiOBr (3:1),其中ZnO/BiOBr (1:2)的降解速率常数最大,为 0.04050 min^{-1} ,是纯BiOBr的4倍。从图6(d)中清楚地看到ZnO/BiOBr (1:2)作用下,随光照时间(min)延长,罗丹明B溶液的颜色由鲜亮逐渐变为黄色直至变为无色,由此可判断罗丹明B基本完全降解。

2.3 重复利用实验

重复利用实验结果显示(图7),将ZnO/BiOBr (1:2)重复降解罗丹明B 5次后仍保持较高的活性,罗丹明B的降解率下降了9%,说明复合光催化剂ZnO/BiOBr (1:2)具有良好的稳定性。

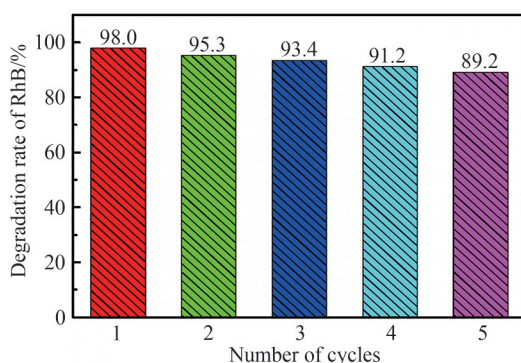


图7 重复利用实验
Fig.7 Reuse experiment

2.4 光催化降解罗丹明B的机理探究

为了确认可见光照射下ZnO/BiOBr (1:2)二元复合光催化剂的活性物种,引入了ESR分析。如图8(a)和(b)所示,在黑暗环境下没有发现 $\cdot\text{O}^{2-}$ 和 $\cdot\text{OH}$ 信号。引入可见光照射,出现明显的DMPO- $\cdot\text{O}^{2-}$ 和DMPO- $\cdot\text{OH}$ 衍射信号。而且随着光照时间增强(光照5 min和10 min),衍射信号明显增强,说明随着光照时间的延长,ZnO/BiOBr (1:2)光催化反应体系中会产生更多的 $\cdot\text{O}^{2-}$ 和 $\cdot\text{OH}$ 自由基。EPR结果表明,ZnO/BiOBr (1:2)光催化体系中确实产生了大量的 $\cdot\text{O}^{2-}$ 和 $\cdot\text{OH}$ 自由基。因此可初步断定 $\cdot\text{O}^{2-}$ 和 $\cdot\text{OH}$ 自由基是ZnO/BiOBr (1:2)光催化反应体系中重要的活性物种^[11]。

为了进一步确定光催化降解机理,引入半导体能带理论分析,根据半导体的禁带宽度 E_g ,可以计算得出半导体的导带(CB)和价带(VB)的位置,即^[16]

$$E_{\text{CB}} = X - E_c - 0.5E_g \quad (4)$$

$$E_{\text{VB}} = E_g + E_{\text{CB}} \quad (5)$$

式中, E_{VB} 表示价带的电位, E_{CB} 表示导带的电位, E_c 为氢尺度上自由电子的能量($\sim 4.5 \text{ eV}$), X 表示电负性,通过计算ZnO和BiOBr的电负性分别为5.79 eV和6.206 eV,通过紫外-可见漫反射估算出ZnO和BiOBr的 E_g 分别为3.21 eV和2.80 eV,计算得到ZnO的导带和价带的位置分别为 -0.31 eV 和 2.89 eV ,BiOBr的导带和

价带的位置分别为0.31 eV和3.11 eV。

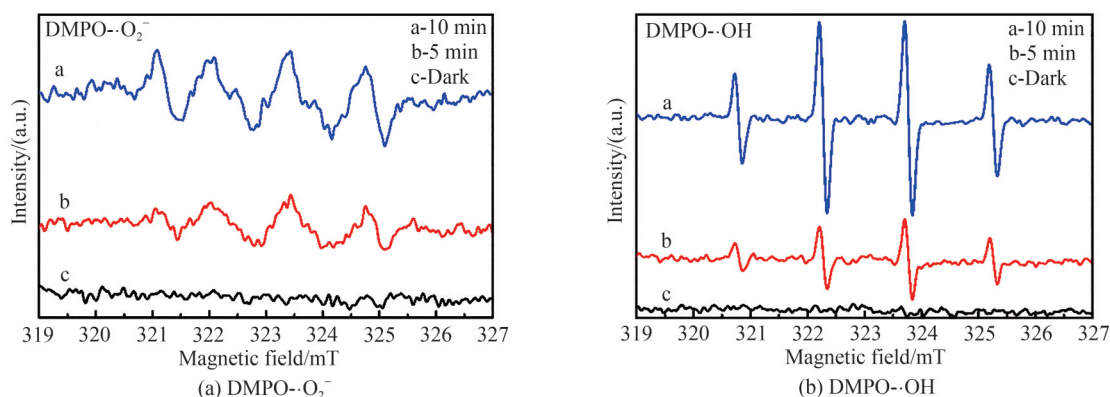


图8 可见光下催化剂ZnO/BiOBr(1:2)的ESR谱
Fig.8 EPR spectra for ZnO/BiOBr (1:2) under visible-light irradiation with

如图9所示,当系统受到可见光照射时($\lambda > 400$ nm,能量小于3.10 eV),对于RhB分子而言会被激发产生 e^- 和 RhB^{*+} , RhB^{*+} 不稳定,可进一步分解成小分子,直至降解,但是在没有其他电子受体的情况下, e^- 和 RhB^{*+} 可快速复合,因此RhB在光照下几乎不能分解^[16]。在本光催化系统中,ZnO CB的边缘高于RhB LUMO边缘,因此电子会自动迁移到ZnO CB的位置,从而实现 RhB^{*+} 进一步降解。

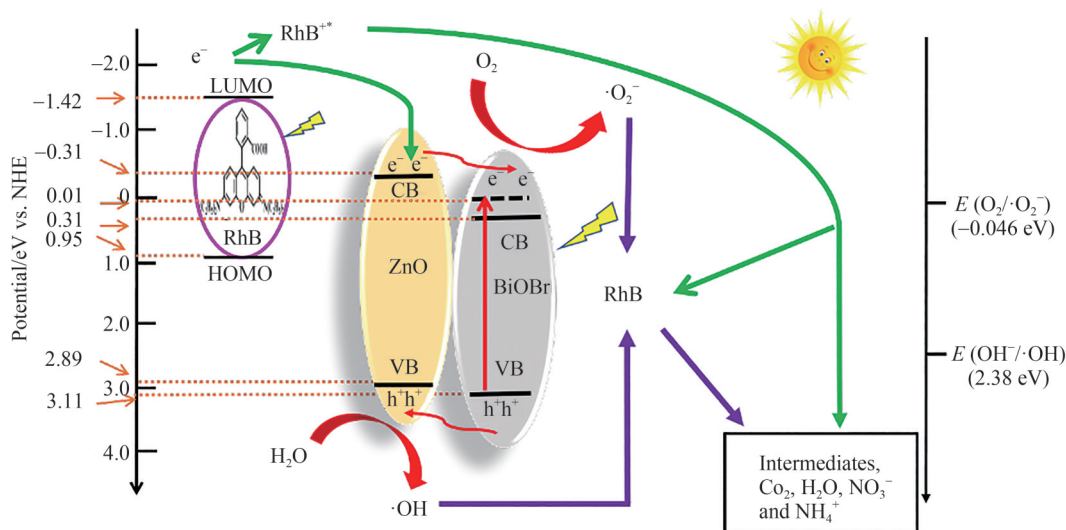
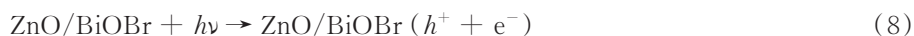
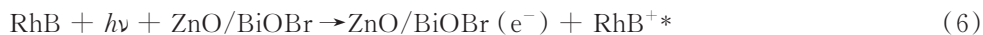


图9 ZnO/BiOBr(1:2)光催化降解机理
Fig.9 Photocatalytic degradation mechanism of ZnO/BiOBr (1:2)

对于光催化剂而言,可见光子的能量小于ZnO禁带宽度(3.21 eV),从而ZnO VB上的电子不会被激发,而光子的能量大于BiOBr的禁带宽度(2.80 eV),因此BiOBr VB中的电子(e^-)被激发到CB中,且可被激发到更高的电位(-0.49 eV),与之对应于VB产生空穴(h^+)^[17-18]。由于BiOBr的CB底部高于ZnO的CB底部,因此ZnO CB上的电子会自动转移到BiOBr CB位置,进而在ZnO的VB处产生空穴。由于ZnO的VB边缘低于BiOBr的VB边缘,因此BiOBr VB上的空穴自动转移到ZnO的VB位置,这样就在复合光催化剂ZnO/BiOBr上形成了一个交错循环的能带结构,进而形成界面电场^[19]。这种结构可以增强 e^- 和 h^+ 的转移,避免两者的复合。接下来是自由基的形成,ZnO CB中的电子被 O_2 捕获,生成 $\cdot O_2^-$,BiOBr VB上的空穴被 H_2O 捕获产生 $\cdot OH$,与EPR分析结果一致,具有强氧化性的 $\cdot O_2^-$ 、 $\cdot OH$ 自由基可将RhB分子或 RhB^{*+} 分解为 CO_2 、 H_2O 、 NO_3^- 和 NH_4^+ ^[20]。 $\cdot O_2^-$ 、 $\cdot OH$ 自由基是无选择性氧化物质,因此可将ZnO/BiOBr(1:2)催化剂应用到其他有机物的降解,用于处理有机废水。

通过以上分析,ZnO/BiOBr(1:2)光催化降解RhB的机理可表示为



3 结论

本文采用溶剂热法合成不同摩尔配比的二元复合材料 ZnO/BiOBr, 其中 ZnO/BiOBr (1:2) 光催化剂降解 RhB 的能力最佳, 光照 120 min, 罗丹明 B 的降解速率达到 98.89%, 一级反应速率常数为 0.0405 min^{-1} ; ZnO 与 BiOBr 复合后, 较纯 ZnO, 禁带宽度变窄, 吸收边带红移, 对光的吸收能力增强, 且光生电子-空穴的复合机率减小; ZnO/BiOBr (1:2) 光催化过程中形成界面电场, 抑制光生电子-空穴的复合, 降解 RhB 过程主要通过 $\cdot\text{O}_2^-$ 、 $\cdot\text{OH}$ 自由基氧化作用。

参考文献

- [1] MIN G, JI E, KANG S, et al. Photocatalytic degradation of methylene blue under UV and visible light by brookite-rutile Bi-crystalline phase of TiO_2 [J]. *New Journal of Chemistry*, 2021, 45: 3485-3497.
- [2] LIU Wenfei, ZHAO Yingjie, LI Huiting, et al. Ag deposition on N and B Co-doped TiO_2 nanoparticles: an avenue for high-efficiency photocatalytic degradation of dye and hydrocarbons in oil-contaminated wastewater [J]. *Nano*, 2021, 16(4): 2150042.
- [3] LIU Yang, HU Zhuofeng, JIMMY C. Photocatalytic degradation of ibuprofen on S-doped BiOBr [J]. *Chemosphere*, 2021, 278(1):130376.
- [4] FUJISHIMA A, HONDA K. Electrochemical photolysis of water at a semiconductor electrode [J]. *Nature*, 1972, 238 (5358): 37-38.
- [5] LIU Kun, QIN Yuelong, MUHAMMAD Y, et al. Effect of Fe_3O_4 content and microwave reaction time on the properties of $\text{Fe}_3\text{O}_4/\text{ZnO}$ magnetic nanoparticles [J]. *Journal of Alloys and Compounds*, 2019, 781: 790-799.
- [6] GENG Yanling, LI Na, MA Jiyan, et al. Preparation, characterization and photocatalytic properties of BiOBr/ZnO composites [J]. *Journal of Energy Chemistry*, 2017(3):416-421
- [7] TONG Zhifang, HE Lingling, REN Chunguang, et al. One-step calcination preparation of worm-like heterojunction with enhanced visible light response for mild photooxidation reaction [J]. *Materials Letters*, 2018, 217(15):296-299.
- [8] YIN Weiqing, CAO Xujing, WANG Bin, et al. In-situ synthesis of $\text{MoS}_2/\text{BiOBr}$ material via mechanical ball milling for boosted photocatalytic degradation pollutants performance [J]. *Chemistry Select*, 2021, 6(5):928-936.
- [9] YANG Hao, ZHANG Qingxia, CHEN Ying, et al. Ultrasonic-microwave synthesis of ZnO/BiOBr functionalized cotton fabrics with antibacterial and photocatalytic properties [J]. *Carbohydrate Polymers*, 2018, 201:162-171.
- [10] SHASHA Y, ZHAO Fei, YUE Xinzhen, et al. Enhanced solar light-driven photocatalytic activity of BiOBr-ZnO heterojunctions with effective separation and transfer properties of photo-generated chargers [J]. *New Journal of Chemistry*, 2015, 8:1-8.
- [11] GENG Yanli, LI Na, MA Jiyan, et al. Preparation, characterization and photocatalytic properties of BiOBr/ZnO composites [J]. *Journal of Energy Chemistry*, 2017, 3:416-421.
- [12] MENG Xiangchao, JIANG Lingyun, WANG Weiwen, et al. Enhanced photocatalytic activity of BiOBr/ZnO heterojunction semiconductors prepared by facile hydrothermal method [J]. *International Journal of Photoenergy*, 2015, 2015:1-9.
- [13] WANG Zhumei, LI Yueming, LIAO Runhua, et al. Preparation and photocatalytic properties of NiO/ TiO_2 nanotubes by hydrothermal method [J]. *Acta Photonica Sinica*, 2019, 48(3): 0316003.
王竹梅, 李月明, 廖润华, 等. NiO/ TiO_2 复合纳米管的水热制备及光催化性能 [J]. *光子学报*, 2019, 48(3): 0316003.
- [14] ZHOU Yujian, YANG Xue, YANG Jikai, et al. Preparation and photoelectrocatalytic properties of WO_3/Pt composite [J]. *Acta Photonica Sinica*, 2021, 50(3): 0331002.
周玉鉴, 杨雪, 杨继凯, 等. WO_3/Pt 复合薄膜的制备及其光电催化性能 [J]. *光子学报*, 2021, 50(3): 0331002.
- [15] CHANG Junqing, ZHONG Yan, HU ChaoHao, et al. Study on highly efficient BiOCl/ZnO p-n heterojunction: synthesis, characterization and visible-light-excited photocatalytic activity [J]. *Journal of Molecular Structure*, 2019, 1183 (5): 209-216.
- [16] LI Jianhui, YANG Fan, ZHOU Quan, et al. A regularly combined magnetic 3D hierarchical $\text{Fe}_3\text{O}_4/\text{BiOBr}$ heterostructure: fabrication, visible-light photocatalytic activity and degradation mechanism [J]. *Journal of Colloid and*

- Interface Science, 2019, 546:139-151.
- [17] GAO Shengwang, GUO Changsheng, HOU Song, et al. Photocatalytic removal of tetrabromobisphenol a by magnetically separable flower-like BiOBr/BiOI/Fe₃O₄ hybrid nanocomposites under visible-light irradiation[J]. Journal of Hazardous materials, 2017, 331(5): 1-8.
- [18] PRASHANTH V, PRIYANKA K, REMYA N. Solar photocatalytic degradation of metformin by TiO₂ synthesized using Calotropis gigantea leaf extract[J]. Water Science and Technology, 2021, 83(3):1-12.
- [19] HAO Xueli, YU Xiujuan, LI Haiying, et al. The preparation of full-range BiOBr/BiOI heterojunctions and the tunability of their photocatalytic performance during the synthesis of imines under visible light irradiation [J]. Applied Surface Science, 2020, 528:147015-147024.
- [20] KHALID N R, MAZIA U, TAHIR M B, et al. Photocatalytic degradation of RhB from an aqueous solution using Ag₃PO₄/N-TiO₂ heterostructure[J]. Journal of Molecular Liquids, 2020, 313:113522-113530.

Preparation of ZnO/BiOBr Composites and Photocatalytic Degradation of RhB under Visible Light

LI Jianhui¹, YANG Chunmei¹, ZHANG Caifeng^{1,2}, ZHANG Shen¹, MA Xiaohong¹,
WU Xiaojing¹, WANG Tainye¹, YUE Xiuli¹, CHANG Minran¹

(1 Department of Chemistry, Taiyuan Normal University, Jinzhong, Shanxi 030619, China)

(2 Engineering Research Center of Organic Dryland Farming Fertilizer of Shanxi Province, Jinzhong, Shanxi 030619, China)

Abstract: In the process of industrial production activities such as textile, printing and dyeing, coating and medicine, about 10%~15% of organic pollutants will be discharged into the surrounding water, soil and atmosphere with industrial wastewater, which increases the difficulty of organic dye treatment. Photocatalysis is considered to be one of the most promising technologies to solve the problems of energy shortage and environmental pollution in the future. It has been used to degrade organic pollutants. However, there are still many problems in the application of photocatalysts, such as low photon efficiency, high recombination rate of photoinduced electron hole pairs or poor stability. In order to expand the industrial application of photocatalytic technology, the modification of photocatalyst is an important direction to improve the utilization of solar energy. ZnO has the advantages of good photosensitivity, non toxicity, high electron mobility and low cost, but it is a wide band gap semiconductor, only responds to ultraviolet light, and the photon utilization is low. Bismuth oxyhalide BiOX (X=Cl, Br, I) has attracted extensive attention because of its special structure and excellent photocatalytic performance. As a typical bismuth halide oxide photocatalyst, BiOBr has a suitable band gap (2.61 eV), which makes it have the characteristics of good activity and stable photocatalytic performance under visible light irradiation. Therefore, it has become one of the materials that can not be ignored in the field of photocatalytic degradation of water pollution. However, the photocatalytic effect of pure BiOBr is poor. The combination of BiOBr and ZnO to form ZnO/BiOBr heterojunction can improve the photocatalytic activity of single component semiconductor photocatalytic materials and broaden the application range of ZnO and BiOBr. In previous studies, the binary composite ZnO/BiOBr was synthesized by hydrothermal method, and the dye degradation experiment was carried out to improve the photocatalytic degradation activity of single component. SHASHA Y et al. prepared ZnO/BiOBr complex by two-step hydrothermal method and showed excellent catalytic activity for the photodegradation of Methyl Orange (MO). GENG Y G et al. synthesized flower like ZnO/BiOBr by hydrothermal method, showing good photocatalytic degradation ability for Methyl Blue (MB). MENG X C et al. synthesized binary heterojunction ZnO/BiOBr by hydrothermal method. The photodegradation ability of Rhodamine B (RhB) was obviously better than that of single component. In previous studies, ZnO/BiOBr binary composites were synthesized by hydrothermal method, and some were synthesized by two-step method. This subject tried to synthesize ZnO/BiOBr with different morphology in one step by adding some ethylene glycol solvent. Although the photocatalytic activity could not be compared with previous studies due to different reaction conditions and degradation substrates, ZnO/BiOBr (1:2) with high catalytic degradation activity was selected in this work. ZnO/

BiOBr composite photocatalysts with different ratios of ZnO and BiOBr (1:1, 1:2, 1:3, 2:1, 2:3, 3:1 and 3:2) were prepared. When the molar ratio of ZnO to BiOBr was 1:2, the photocatalytic degradation performance of ZnO/BiOBr composite was the best. Under visible light for 120 min, the removal rate of Rhodamine B (RhB) (20 mg/L) was 98.89% and the degradation rate constant was $0.040\ 50\ \text{min}^{-1}$, which was 4 times that of pure BiOBr. The binary composites ZnO/BiOBr were detected through X-ray diffraction, scanning electron microscopy, transmission electron microscopy, high resolution TEM, UV-vis diffuse reflection spectroscopy, photoluminescence analysis and electron spin resonance spectroscopy. X-ray diffraction analysis and transmission electron microscope analysis found that ZnO and BiOBr were successfully compounded. The scanning electron microscope analysis results showed that the binary composite ZnO/BiOBr with different molar ratios showed flake structures of different sizes, and granular ZnO could not be seen on the surface of flake structures. Among them, the flake structure size of ZnO/BiOBr (1:2) sample was the largest. UV-vis diffuse reflectance analysis showed that compared with pure ZnO, the band gap decreased significantly after BiOBr and ZnO were combined, indicating that the utilization range of spectrum was improved, which was beneficial to the improvement of photocatalytic performance. Photoluminescence analysis showed that the peak intensity of ZnO/BiOBr (1:2) binary composite was between pure ZnO and BiOBr, indicating that the addition of BiOBr improved the utilization of photogenerated electrons and holes in pure ZnO. The results of reuse experiment showed that after repeatedly degrading Rhodamine B (RhB) 5 times, ZnO/BiOBr (1:2) still maintained high activity, and the degradation rate of Rhodamine B decreased by 9%, indicating that the composite photocatalyst ZnO/BiOBr (1:2) had good stability. Electron spin resonance spectroscopy results showed that a large number of $\cdot\text{O}_2^-$ and $\cdot\text{OH}$ radicals were indeed produced in ZnO/BiOBr (1:2) photocatalytic system. Therefore, it could be preliminarily concluded that $\cdot\text{O}_2^-$ and $\cdot\text{OH}$ radicals were important active species in ZnO/BiOBr (1:2) photocatalytic reaction system. Combined with the theoretical analysis of semiconductor energy band, the existence of $\cdot\text{O}_2^-$ and $\cdot\text{OH}$ radicals was confirmed again, and the organics were degraded into small molecular substances through their oxidation. The photocatalytic degradation mechanism showed that the interface electric field was formed in the photocatalytic process of ZnO/BiOBr (1:2) to inhibit the recombination of photogenerated electrons and holes. All results suggested that the ZnO/BiOBr (1:2) composite with high photocatalytic degradation efficiency, excellent recyclability and stability can meet a potentially promising application for photocatalytic degradation of waste water.

Key words: Photocatalysis; Photon; Degradation; ZnO/BiOBr; Rhodamine B

OCIS Codes: 160.6000; 160.4760; 350.6050; 160.4236